



Cite this: *Chem. Sci.*, 2019, 10, 4192

All publication charges for this article have been paid for by the Royal Society of Chemistry

# Construction of a cross-layer linked G-octamer via conformational control: a stable G-quadruplex in H-bond competitive solvents†

Ying He,<sup>‡a</sup> Yanbin Zhang,<sup>‡b</sup> Lukasz Wojtas,<sup>a</sup> Novruz G. Akhmedov,<sup>c</sup> David Thai,<sup>a</sup> Heng Wang,<sup>a</sup> Xiaopeng Li,<sup>a</sup> Hao Guo<sup>ID</sup>\*<sup>b</sup> and Xiaodong Shi<sup>ID</sup>\*<sup>a</sup>

Methanol soluble and stable guanosine octamers were successfully achieved via H-bond self-assembly. Through structural conformational design, we developed a new class of guanosine derivatives with modification on guanine (8-aryl) and ribose (2',3'-isopropylidene). This unique design led to the formation of the first discrete G<sub>8</sub>-octamer with its structure characterized by single crystal X-ray diffraction, MS and NMR spectroscopy. The G<sub>8</sub>-octamer showed unique cation recognition properties, including the formation of a stable Rb<sup>+</sup> templated G-quadruplex. Based on this observation, further modification on the 8-aryl moiety was performed to incorporate a cross-layer H-bond or covalent linkage. Similar G-octamers were obtained in both cases with structures confirmed by single crystal X-ray diffraction. Furthermore, the covalently linked G-quadruplex exhibited excellent stability even in MeOH and DMSO, suggesting a promising future for this new H-bond self-assembly system in biological and material applications.

Received 12th January 2019

Accepted 5th March 2019

DOI: 10.1039/c9sc00190e

rsc.li/chemical-science

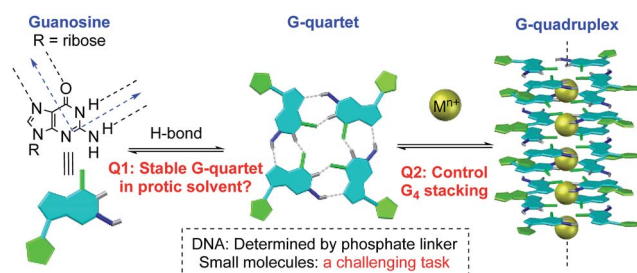
## Introduction

Non-covalent interactions enable construction of large structural motifs from small molecules.<sup>1–3</sup> Molecular self-assembly, an important process typically driven by non-covalent interactions, is often dynamic and generally under thermodynamic control.<sup>4,5</sup> With interest in the application of the self-assembly process to biomedical research, there is a growing demand with respect to preparing stable non-covalent assemblies in a biocompatible environment.<sup>6–8</sup> However, supramolecular structures built through H-bonds are often studied in less polar aprotic solvents (such as CH<sub>2</sub>Cl<sub>2</sub>) to avoid the competition of H-bond interactions between substrates and solvents.<sup>9,10</sup> Thus, the development of novel supramolecular systems which are stable in a polar protic solvent is highly desirable, though very challenging.<sup>11,12</sup>

A G-quartet is an interesting supramolecular scaffold formed by H-bonds.<sup>13,14</sup> As shown in Scheme 1, with an approximately 90-degree angle between the H-bond donor and acceptor, four

guanine units are held together to form a G-quartet. Through ion–dipole interactions, alkali and alkaline earth metal cations can enhance the process by serving as the template to coordinate with central oxygen atoms.<sup>15–17</sup> Stacking of G-quartets gives G-quadruplexes as bioactive building blocks found in DNA and RNA folding.<sup>18,19</sup> In this case, the extent of G-quartet stacking in a G-quadruplex will be determined by the phosphate backbone, which is often associated with the formation of a counter folding subunit, such as the i-motif.<sup>20</sup>

Inspired by this unique H-bond assembly, researchers have been devoted to developing guanine derivatives to achieve controllable G-quadruplex formation from small molecules.<sup>21–23</sup> Some interesting applications have been identified with various G-quartet assemblies, including lipophilic ion channels,<sup>24–26</sup> supramolecular hydrogels,<sup>27–29</sup> nanomaterials,<sup>30,31</sup> potential targets for cancer therapy,<sup>32,33</sup> and more.<sup>34–37</sup> Although many examples of G-quartet formation through various modified



Scheme 1 G-quadruplex formation: equilibrium and stability.

<sup>a</sup>Department of Chemistry, University of South Florida, 4202 E. Fowler Avenue, Tampa, Florida 33620, USA. E-mail: xmshi@usf.edu

<sup>b</sup>Department of Chemistry, Fudan University, 2005 Songhu Road, Shanghai, 200438, People's Republic of China

<sup>c</sup>Department of Chemistry, West Virginia University, Morgantown, WV 26505, USA

† Electronic supplementary information (ESI) available: Experimental section, NMR spectra, ESI-MS spectra and crystallographic data. CCDC 1871565–1871570 and 1871754. For ESI and crystallographic data in CIF or other electronic format see DOI: 10.1039/c9sc00190e

‡ Equal contribution.



guanine derivatives have been reported, studies on controlling G-quartet stacking molecularly are relatively rare.<sup>38,39</sup> Factors to be taken into consideration include the cation concentration,<sup>39</sup> the solvent,<sup>40</sup> the anion,<sup>41</sup> and so on.<sup>42</sup> In many cases, mixtures of various “stacking isomers” ( $G_8$ ,  $G_{12}$  or  $G_{16}$ ) were observed, which highlights the significant challenges associated with controlling the vertical stacking.<sup>43–46</sup> Moreover, the assembly of a specific and stable G-quadruplex in H-bond competitive solvents remains a challenging task.<sup>48</sup> Herein, we report the construction of the first G-octamer with structures characterized by single crystal X-ray diffraction through monomer conformational design. Moreover, with this new system, stable G-quadruplexes were formed with significantly improved stability. Through the design of cross-layer H-bonds and covalent linkage, G-octamers were prepared with excellent stability in MeOH (no dissociation) and even in 50% DMSO, which offers a potential opportunity to extend the H-bond assembly system into biosystems for future applications.

## Results and discussion

### Design, synthesis and characterization of G-octamers

Ideally, a  $G_4$ -tetramer would be the most concise target towards the construction of a simple and stable assembled structure. However, with a metal template in solution, further stacking of  $G_4$ -tetramers leads to the mixture of G-quadruplex species.<sup>49</sup> Thus,  $G_4$ -tetramers are unfavorable for the formation of well-defined supermolecules.

The simplest plausible G-quadruplex would be a G-octamer which is likely to adopt either top-to-top (T-T) or bottom-to-bottom (B-B) stacking patterns (Scheme 2A).<sup>50</sup> In previous

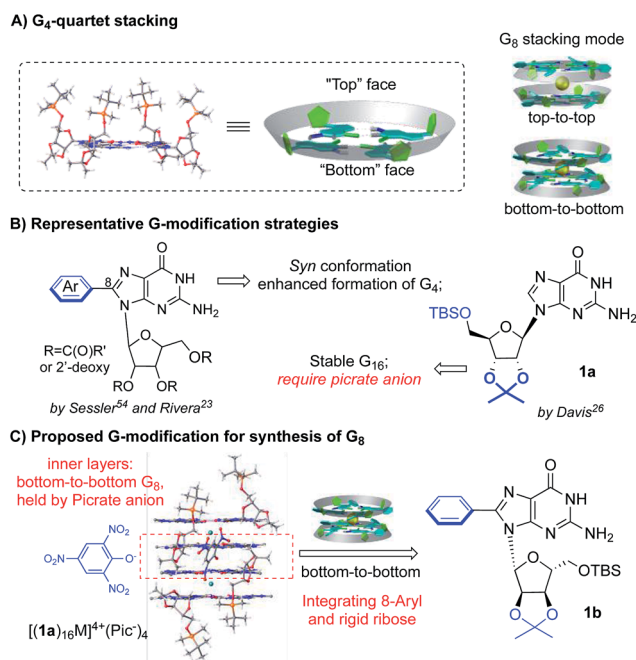
studies, Meijer *et al.* employed different concentrations of a guanosine derivative resulting in the formation of tunable G-octamers.<sup>41</sup> Spada has reported G-octamer formation upon exposure to UV light through alkene isomerization.<sup>51</sup> Wu presented several excellent examples of G-octamer formation through  $\pi$ - $\pi$  interactions using NMR and MS studies.<sup>52</sup> Hirao and coworkers applied Au(I)-Au(I) interaction between two G-quartet layers to achieve a G-octamer confirmed by NMR and CD spectra.<sup>53</sup> However, to the best of our knowledge, no single crystal structure of a G-octamer has ever been reported, implying the challenging nature of preparing a stable and discrete G-octamer in a dynamic equilibrium.

To tackle this problem, we set out to design a G-derivative where the structure is rigid and predisposed for the conformation of a potential octamer structure so as to minimize the entropy cost involved in the self-assembly process. As shown in Scheme 2B, modification of guanosine often occurs on two positions: C-8 of purine and the hydroxyl of ribose. The Sessler group first reported on 8-aryl substituted guanosine in the formation of a G-quartet without templating cation in both solution and solid state.<sup>54</sup>

This seminal work initiated the concept of conformational control for G-quartet formation: the steric effect between the aryl substituent and protected ribose helped guanosine to adopt a *syn* conformation, preventing the ribbon formation and giving a tetramer as the dominant conformation. On the other hand, Davis's group developed lipophilic guanosine with bulky ribose to form a G-hexadecamer (Scheme 2B) both in solution and solid state ( $M^{n+} = K^+$ ,  $Ba^{2+}$ ,  $Sr^{2+}$ , and  $Pb^{2+}$ ).<sup>55</sup> Notably, a picrate anion bridge played a crucial role: as revealed by single crystal X-ray diffraction (Scheme 2C), four picrate anions linked two G-octamers through H-bonds between anion and two inner G-quartets. The two G-octamers (from adjacent inner and outer  $G_4$ ) gave top-to-bottom stacking with ribose interdigitated between the adjacent layers. Interestingly, the two inner layers adopted bottom-to-bottom (B-B) stacking, which is more favorable than the T-T mode with the cation binding on the more “naked” convex face between the two layers. This result aroused our interest in developing a G-octamer through similar B-B stacking.

Considering the steric interaction between the C-8 substituent and ribose, we postulated that incorporation of C-8 aryl and the rigid ribose ring might provide a new system with steric hindrance between the G-quartet to force the  $G_4$  bowls to stack in a bottom-to-bottom manner, while obstructing ribose interdigitation at the top-face (Scheme 2C). To confirm this idea, compound **1b** was designed, prepared and applied to assemble with various alkali and alkaline earth metal cations. <sup>1</sup>H NMR spectra were obtained and selected regions of the <sup>1</sup>H NMR spectra of these G-quadruplexes were compared with the G-hexadecamer from **1a** as shown in Fig. 1.

As previously reported, treating **1a** with alkali and alkaline earth metal salts ( $K^+$ ,  $Ba^{2+}$ ,  $Sr^{2+}$  and so on) gave two sets of signals in the <sup>1</sup>H NMR spectra, corresponding to the inner and outer G-quartet.<sup>56</sup> Conducting similar cation binding experiments with **1b** in  $CDCl_3$  gave a single set of <sup>1</sup>H NMR signals in all cases ( $M = K^+$ ,  $Ba^{2+}$ , and  $Sr^{2+}$ ;  $A^- = Picrate^-$  or  $PF_6^-$ ). Furthermore, ESI-MS demonstrated a clear doubly charged



Scheme 2 Achieving a stable G-octamer by controlling G-quartet stacking.



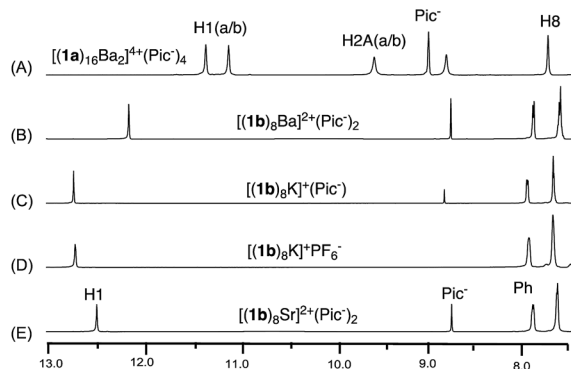


Fig. 1  $^1\text{H}$  NMR spectra of G-quadruplexes (A)  $[(\mathbf{1a})_{16}\text{Ba}_2]^{4+} \cdot (\text{Pic}^-)_4$ ; (B)  $[(\mathbf{1b})_8\text{Ba}]^{2+} \cdot (\text{Pic}^-)_2$ ; (C)  $[(\mathbf{1b})_8\text{K}]^+ \cdot (\text{Pic}^-)$ ; (D)  $[(\mathbf{1b})_8\text{K}]^+ \cdot (\text{PF}_6^-)$ ; (E)  $[(\mathbf{1b})_8\text{Sr}]^{2+} \cdot (\text{Pic}^-)_2$  in  $\text{CDCl}_3$ .

peak at  $m/z = 2123.01$ , corresponding to a mol. wt of 4246.68 for  $[(\mathbf{1b})_8\text{Ba}]^{2+}$ . The experimental and calculated isotope patterns further suggested an octameric composition. In addition, traveling wave ion mobility-mass spectrometry (TWIM-MS)<sup>57</sup> confirmed no formation of stacking isomers, which excluded the formation of random aggregates in gas phase (see ESI† for details).

Finally, single crystal structures were obtained and unambiguously verified the  $\text{G}_8$ -octamer formation with the proposed bottom-to-bottom stacking (Fig. 2A). The top view of the crystal structure (Fig. 2B) shows the G-quartet self-assembly in the tail to tail orientation. The five crystal structures obtained with ligand  $\mathbf{1b}$  include monovalent cations ( $\text{K}^+$  and  $\text{Rb}^+$ ) and divalent cations ( $\text{Ba}^{2+}$  and  $\text{Sr}^{2+}$ ). Picrate anion showed no clear binding with the G-quartet, consistent with what was observed in the  $^1\text{H}$  NMR spectra (see Fig. S2†). A complex with non-coordinated  $\text{PF}_6^-$  anion was also successfully obtained,  $[(\mathbf{1b})_8\text{K}]^+ \cdot (\text{PF}_6^-)$ , confirming the “anion-free” binding mode of this new type of  $\text{G}_8$ -quadruplex. The distances of the H-bond within the  $\text{G}_4$ -quartet and between the  $\text{G}_4$  layers are compared in Table 1.

According to these crystal structures, all  $\text{G}_8$ -octamers from  $\mathbf{1b}$  gave  $\text{G}_4$ -quartets with an (N1...O6) and (N2...N7) H-bond distance of around 2.9 Å, similar to that of the inner and outer layer in the  $\text{G}_{16}$ -hexadecamer formed from  $\mathbf{1a}$ .<sup>46</sup> These results indicated that both cations and the C-8 phenyl substituent had little influence on the H-bond in the  $\text{G}_4$ -quartet.

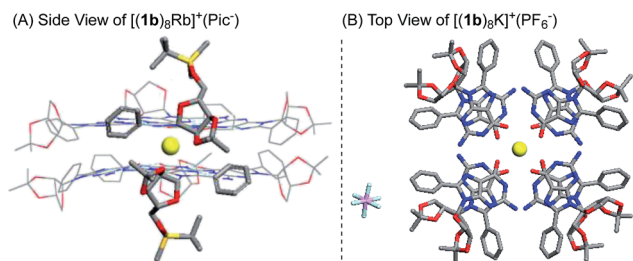


Fig. 2 X-ray single crystal structure of the  $\text{G}_8$ -octamer (A)  $[(\mathbf{1b})_8\text{Rb}]^+ \cdot (\text{Pic}^-)$ ; (B)  $[(\mathbf{1b})_8\text{K}]^+ \cdot (\text{PF}_6^-)$ . Similar structures for  $[(\mathbf{1b})_8\text{K}]^+ \cdot (\text{Pic}^-)$ ,  $[(\mathbf{1b})_8\text{Ba}]^{2+} \cdot (\text{Pic}^-)_2$  and  $[(\mathbf{1b})_8\text{Sr}]^{2+} \cdot (\text{Pic}^-)_2$  were also obtained.†

However, the size of the  $\text{G}_8$  was influenced by the average O–M distances of all these complexes from  $\mathbf{1b}$ , which might follow the trend where higher ionic potential ( $Z/r$ ) resulted in shorter O–M distance (2.75–2.81 Å). Interestingly, in comparison with the  $\text{G}_{16}$ -hexadecamer  $[(\mathbf{1a})_{16}\text{Ba}_2]^{4+} \cdot (\text{Pic}^-)_4$ , the  $\text{G}_8$ -octamers  $[(\mathbf{1b})_8\text{Ba}]^{2+} \cdot (\text{Pic}^-)_2$  gave a slightly shorter distance between the two  $\text{G}_4$  layers (2.89 Å vs. 3.06 Å and 3.58 Å). This result implied the stronger cation interaction of the  $(\mathbf{1b})_4$ -quartet than the  $(\mathbf{1a})_4$ -quartet. This improved cation interaction has been supported by  $\text{G}_4$ -binding studies with  $\text{Rb}^+$  using the  $\mathbf{1b}$  ligand and led to the first crystal structures of  $\text{Rb}^+$  coordinated  $\text{G}$ -quadruplexes. Among all the  $\text{G}_8$  crystals,  $[(\mathbf{1b})_8\text{Rb}]^+ \cdot (\text{Pic}^-)$  gave the longest O–M and  $\text{G}_4$ – $\text{G}_4$  distance due to its large radii<sup>58</sup> and low valency. Very few examples of  $\text{Rb}$  coordinated  $\text{G}$ -quartets have been reported so far, indicating how challenging it is for guanosine to bind with  $\text{Rb}$  to form a discrete  $\text{G}$ -quadruplex.<sup>59</sup> To the best of our knowledge, this is the first single crystal structure of a  $\text{G}$ -quadruplex containing  $\text{Rb}^+$ , clearly suggesting the promising cation binding ability of guanosine derivative  $\mathbf{1b}$ .

Having successfully confirmed a new concise  $\text{G}_8$ -quadruplex structure in solution (NMR), solid state (XRD) and gas phase (ESI-MS and TWIM-MS), we evaluated its stability in MeOH. Dissolving octamer  $[(\mathbf{1b})_8\text{K}]^+ \cdot (\text{Pic}^-)$  in  $\text{CD}_3\text{OD}$  gave a mixture of two sets of signals in NMR spectra, suggesting partial decomposition of this  $\text{G}_8$ -octamer (*vide infra*). To obtain MeOH stable  $\text{G}$ -quadruplexes, further modification is still needed.

### Cross-layer H-bonded $\text{G}$ -octamers

To further improve the stability of the  $\text{G}$ -quadruplex, we sought to establish the interactions between the  $\text{G}$ -quartet layers. As highlighted in Fig. 2A, the 8-phenyl group in  $\mathbf{1b}$  adopted a tilted conformation and reached out from the  $\text{G}$ -quartet. This geometry provided an opportunity to further enhance the supramolecular structure by introducing new interactions between the two  $\text{G}$ -quartets.

Notably, the Rivera group have reported the formation of an intralayer H-bond between carbonyl oxygen with N(2)H within the same  $\text{G}$ -quartet by using 2'-deoxy guanosine derivatives without rigid ribose functionalization.<sup>34,36–38</sup> This work suggested the possibility of forming extra H-bonds by using both hydrogens of the N(2)– $\text{NH}_2$  group. Inspired by this work, a carbonyl group was introduced at the *meta*-position of the 8-aryl position of  $\mathbf{1b}$  as illustrated in Fig. 3A. Based on this design, we hypothesized that N(2)– $\text{H}_\text{A}$  would form a H-bond with neighboring guanosine within the  $\text{G}$ -quartet, while the N(2)– $\text{H}_\text{B}$  could interact with the carbonyl group by forming a cross-layer H-bond.

To confirm this idea, compound  $\mathbf{1c}$  was synthesized and applied to  $\text{G}$ -quadruplex construction upon interacting with metal cations. According to the  $^1\text{H}$  NMR spectra, treating  $\mathbf{1c}$  with  $\text{Ba}(\text{Pic})_2$  led to the formation of a new  $\text{G}$ -quadruplex with one set of signals, similar to the  $\text{G}_8$ -octamer obtained from  $\mathbf{1b}$ . Analysis of the NMR sample (in  $\text{CDCl}_3$ ) by ESI-MS gave a dominant, doubly charged peak with  $m/z$  at 2291.34, corresponding to  $[(\mathbf{1c})_8\text{Ba}]^{2+}$  ( $m_w = 4582.68$ ).



Table 1 G-quadruplex structural comparison (Å)

G-quadruplex		$d(N1\cdots O6)$	$d(N2\cdots N7)$	$d(O-M)$	$d(G_4-G_4)$
[( <b>1a</b> ) <sub>16</sub> Ba <sub>2</sub> ] <sup>4+</sup> ·(Pic <sup>−</sup> ) <sub>4</sub> <sup>a</sup>	Inner	2.92 ± 0.01	2.91 ± 0.07	2.75 ± 0.02	3.06 (i-o)
	Outer	2.86 ± 0.01	2.89 ± 0.04	2.79 ± 0.03	3.58 (i-i)
[( <b>1b</b> ) <sub>8</sub> K] <sup>+</sup> ·(Pic <sup>−</sup> )		2.82 ± 0.08	2.87 ± 0.04	2.72 ± 0.17	2.85
[( <b>1b</b> ) <sub>8</sub> K] <sup>+</sup> ·(PF <sub>6</sub> <sup>−</sup> )		2.82 ± 0.04	2.89 ± 0.05	2.77 ± 0.03	2.96
[( <b>1b</b> ) <sub>8</sub> Ba] <sup>2+</sup> ·(Pic <sup>−</sup> ) <sub>2</sub>		2.89 ± 0.04	2.89 ± 0.04	2.72 ± 0.05	2.89
[( <b>1b</b> ) <sub>8</sub> Sr] <sup>2+</sup> ·(Pic <sup>−</sup> ) <sub>2</sub>		2.83 ± 0.03	2.86 ± 0.04	2.62 ± 0.05	2.75
[( <b>1b</b> ) <sub>8</sub> Rb] <sup>+</sup> ·(Pic <sup>−</sup> )		2.85 ± 0.03	2.89 ± 0.03	2.81 ± 0.05	3.04

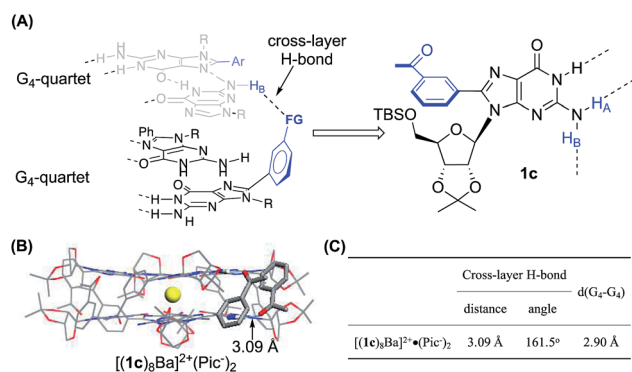
<sup>a</sup> See ref. 46.

Fig. 3 (A) General design of establishing a cross-layer H-bond; (B) single crystal structure and (C) H-bond information of [(**1c**)<sub>8</sub>Ba]<sup>2+</sup>·(Pic<sup>−</sup>)<sub>2</sub>.

Having confirmed the G<sub>8</sub>-octamer [(**1b**)<sub>8</sub>Ba]<sup>2+</sup>·(Pic<sup>−</sup>)<sub>2</sub> formation, our next goal was to determine if there was a cross-layer H-bond as designed above. The <sup>1</sup>H NMR spectra of [(**1b**)<sub>8</sub>Ba]<sup>2+</sup>·(Pic<sup>−</sup>)<sub>2</sub> and [(**1c**)<sub>8</sub>Ba]<sup>2+</sup>·(Pic<sup>−</sup>)<sub>2</sub> did not show peaks corresponding to N(2)H at room temperature. This is likely due to the rapid exchange between the two NH<sub>2</sub> protons, even with the formation of a H-bond. Thus, the exchange rate of the two protons provides a direct indication of the H-bond strength in the G<sub>4</sub>-quartet. To explore the dynamic structure, variable temperature (VT) NMR experiments with [(**1b**)<sub>8</sub>Ba]<sup>2+</sup>·(Pic<sup>−</sup>)<sub>2</sub> and [(**1c**)<sub>8</sub>Ba]<sup>2+</sup>·(Pic<sup>−</sup>)<sub>2</sub> were performed and are summarized in Fig. 4.

For complex [(**1c**)<sub>8</sub>Ba]<sup>2+</sup>·(Pic<sup>−</sup>)<sub>2</sub>, the NH<sub>2</sub> protons started appearing as broad peaks at 0 °C with the chemical shift at 10.28 ppm (H<sub>A</sub>) and 7.25 ppm (H<sub>B</sub>). In contrast, the VT NMR

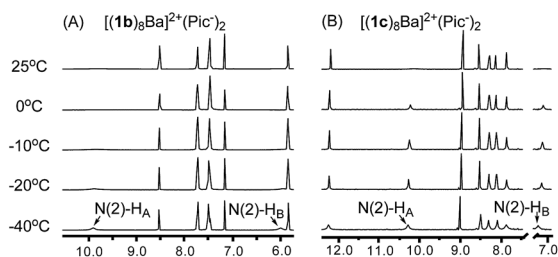


Fig. 4 (A) VT NMR spectra of [(**1b**)<sub>8</sub>Ba]<sup>2+</sup>·(Pic<sup>−</sup>)<sub>2</sub> and (B) VT NMR spectra of [(**1c**)<sub>8</sub>Ba]<sup>2+</sup>·(Pic<sup>−</sup>)<sub>2</sub> confirmed the cross-layer H-bond design in establishing a cross-layer H-bond.

spectra of [(**1b**)<sub>8</sub>Ba]<sup>2+</sup>·(Pic<sup>−</sup>)<sub>2</sub> did not show apparent peaks of the N(2)–H signals until further cooling the sample to −40 °C. The results indicated that there might be an extra H-bond in the **1c** complex to lock the N(2)–NH<sub>2</sub> from rapid exchange. Furthermore, a significantly downfield shifted chemical shift (7.25 ppm) was ascribed to the N(2)–H<sub>B</sub> proton in the (**1c**)<sub>8</sub>-octamer compared with the (**1b**)<sub>8</sub>-octamer (5.98 ppm). These observations provide clear evidence of the formation of a cross-layer H-bond in the (**1c**)<sub>8</sub>-octamer as designed.

Finally, the G<sub>8</sub>-octamer was verified by X-ray crystallography as shown in Fig. 3B. The crystal structure also confirmed the presence of the cross-layer interactions with a mean H-bond distance of 3.09 Å and a bond angle of 161.5°, suggesting a weak cross-layer H-bond present in solid state (Fig. 3C). This makes the structure a “self-assembled molecular-cuboid” purely constructed by H-bond linkage with all eight guanosine units. On the other hand, the distance of the two G-quartet layers (2.90 Å) in [(**1c**)<sub>8</sub>Ba]<sup>2+</sup>·(Pic<sup>−</sup>)<sub>2</sub> remained similar to the **1b** complex. Considering the specific “cage” size in the G<sub>8</sub>-octamer shown in Table 1, the cross-layer H-bond was not strong enough to generate extra enthalpy gain to balance the entropy cost caused by holding the two layers tighter.

With the confirmed cross-layer H-bonds, we evaluated the complex stability of [(**1c**)<sub>8</sub>K]<sup>+</sup>·(Pic<sup>−</sup>) in methanol. The results showed a similar stability to the complex formed with **1b** (*vide infra*). Although the cross-layer H-bond approach could not boost G<sub>8</sub>-quadruplex stability in MeOH as anticipated, it provided an effective and novel approach to enhance G-quadruplex stability from monomer conformational design. Structural amendment was required to further improve the stability of the G<sub>8</sub>-octamer.

### Cross-layer linkage through a covalent bond

To increase the stability to a new level, we turned to establishing a potential covalent linkage between the two G-quartets. By scrutinizing the crystal structure of [(**1b**)<sub>8</sub>Ba]<sup>2+</sup>·(Pic<sup>−</sup>)<sub>2</sub>, we found that the distance between the two *meta* position of the phenyl ring from each tetramer was 4.0 Å, a distance similar to three single bond lengths.<sup>58</sup> According to the observation, the *meta* position of the two phenyl groups could serve as a reference site for constructing cross-layer covalent linkers. The guanosine dimer **1d** and **1d'** were then prepared using the synthetic route summarized in Fig. 5A.



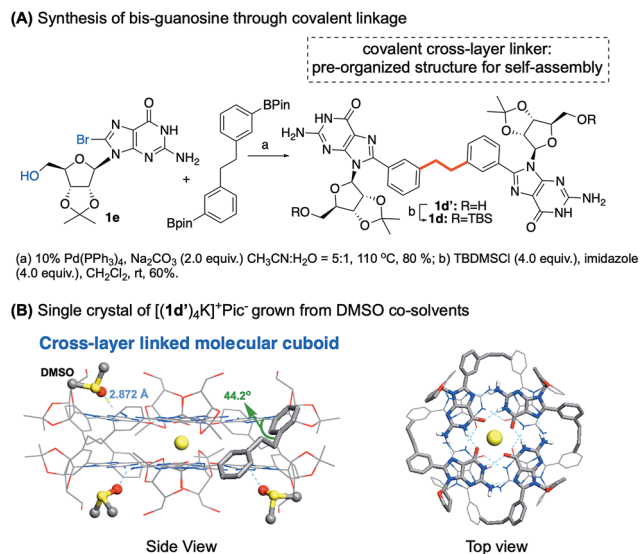


Fig. 5 (A) Synthesis of bis-guanosine derivatives. (B) Single crystal structure of [(1d')<sub>4</sub>K]<sup>+</sup>·(Pic<sup>-</sup>)<sub>2</sub>.

Self-assembly of **1d** with K<sup>+</sup> and Ba<sup>2+</sup> cations in CDCl<sub>3</sub> gave a similar one-set of signals in the <sup>1</sup>H NMR spectra, consistent with the formation of a G<sub>8</sub>-octamer. ESI-MS of complexes from **1d** and Ba<sup>2+</sup> gave a doubly charged peak at *m/z* = 2175.55 as the dominant signal, indicating a mol. wt of 4351.1 for the supermolecule as [(1d)<sub>4</sub>Ba]<sup>2+</sup>. An attempt to obtain a single crystal of the **1d** complex failed initially, resulting in a rather thin, film-like solid formation. Fortunately, the single crystal structure was successfully obtained by switching the monomer to **1d'** using DMSO as a co-solvent, confirming the cross-layer covalent linked structure as proposed (Fig. 5B). Notably, for complex [(1d')<sub>4</sub>Ba]<sup>2+</sup>·(Pic<sup>-</sup>)<sub>2</sub>, the dihedral angle between 8-aryl and guanidine is 40.7 degrees, similar to the dihedral angles in complex [(1b)<sub>8</sub>Ba]<sup>2+</sup>·(Pic<sup>-</sup>)<sub>2</sub> (42.5 degrees). Overall, through G-monomer conformational analysis, a series of G<sub>8</sub>-octamers was successfully prepared with functionalization at 8-phenyl (**1b**), a cross-layer H-bond linker (**1c**) and a covalent linker (**1d**).

### G-quadruplex H-bond stability in MeOH

As discussed above, our intrinsic motivation in exploring these different G-quadruplexes was to develop H-bonded guanosine self-assembly that could survive in protic solvents (H-bond competitive). With all these different G<sub>16</sub> and G<sub>8</sub> quadruplexes prepared, we dissolved them in CD<sub>3</sub>OD to compare the <sup>1</sup>H NMR spectra. As shown in Fig. 6A, N(1)-H and N(2)-H protons did not appear in <sup>1</sup>H NMR spectra with CD<sub>3</sub>OD as the solvent due to the H/D exchange. Thus, evaluation of the <sup>1</sup>H NMR spectra will mainly be focused on the non-exchangeable aromatic protons and ribose protons. Dissolving the G<sub>16</sub>-hexadecamer [(1a)<sub>16</sub>-K<sub>4</sub>]<sup>4+</sup>·(Pic<sup>-</sup>)<sub>4</sub> in CD<sub>3</sub>OD gave only one set of signals, identical to the **1a** monomer in CD<sub>3</sub>OD. The result suggested complete dissociation of the G<sub>16</sub>-hexadecamer to **1a** monomer in MeOH. Interestingly, the G<sub>8</sub>-octamer [(1b)<sub>8</sub>K]<sup>+</sup>·(Pic<sup>-</sup>) and [(1c)<sub>8</sub>-K]<sup>+</sup>·(Pic<sup>-</sup>) in CD<sub>3</sub>OD gave two sets of signals, indicating the existence of dissociated monomer and possible oligomers or

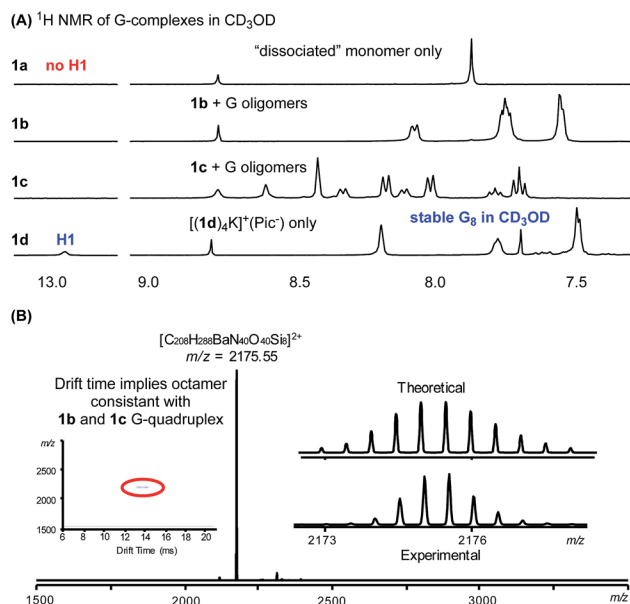


Fig. 6 (A) <sup>1</sup>H NMR spectra showing G-quadruplex stability in CD<sub>3</sub>OD. (B) MS of [(1d)<sub>4</sub>Ba]<sup>2+</sup>·(Pic<sup>-</sup>)<sub>2</sub> in MeOH.

a G-quadruplex in the solution phase. Although the exact structures of the guanosine species in these two cases are not determined at this moment, the fact that H-bonded guanosine complexes were formed with **1b** and **1c** clearly suggests the improved H-binding ability of these two monomers over **1a**. Surprisingly, when dissolving the G<sub>8</sub>-octamer [(1d)<sub>4</sub>K]<sup>+</sup>·(Pic<sup>-</sup>) in CD<sub>3</sub>OD, only one set of signals was observed. Notably, in this case, N(1)-H gave a broad signal at 12.95 ppm, clearly suggesting the formation of a G-quadruplex through a H-bond. NMR solvent signal suppression was applied for the G-quadruplex [(1d)<sub>4</sub>-K]<sup>+</sup>·(Pic<sup>-</sup>) in CD<sub>3</sub>OH. The peak at 12.9 ppm clearly showed up and was confirmed to be H1 of G in the G-quadruplex (see detailed NMR spectra in Fig. S7†). Thus, with monomer **1d**, a G-quadruplex remains intact in protic solvent CD<sub>3</sub>OD. Impressively, this G-quadruplex did not dissociate even at elevated temperature in CD<sub>3</sub>OD, with the N(1)H peak remaining at 60 °C (see Fig. S6† for VT NMR spectra). This observation indicated that there was a high kinetic barrier to break the **1d** G-quartet for H/D exchange, which highlighted the stability of [(1d)<sub>4</sub>K]<sup>+</sup>·(Pic<sup>-</sup>) in a H-bond competitive system. Injecting an MeOH solution of [(1d)<sub>4</sub>-Ba]<sup>2+</sup>·(Pic<sup>-</sup>)<sub>2</sub> complex into ESI-MS gave a dominant double charged peak with *m/z* = 2175.55, corresponding to [(1d)<sub>4</sub>Ba]<sup>2+</sup> (Fig. 6B). It is noteworthy that TWIM-MS of this G-quadruplex in methanol solution was recorded as a single band (*m/z* = 2175.55) with drift time at 14.33 ms, which is in agreement with the size of the G<sub>8</sub>-octamer (see detailed discussion in Table S1†). To the best of our knowledge, this is one of the few stable G-quadruplex systems from small molecule self-assembly to survive in a H-bond competitive environment.

### Evaluating G-quadruplex stability

With the success in maintaining G-quadruplex stability in protic solvent MeOH, we sought to evaluate whether a similar



stability trend exists with polar aprotic solvents. DMSO is a strong polar solvent, which can disrupt the H-bond in G-quartets and cause the decomposition of G-quadruplexes. To evaluate how the incorporation of the phenyl group and cross-layer interaction impact on thermodynamic stability, G-quadruplexes were treated with  $\text{CDCl}_3/\text{DMSO-d}_6$  solvent mixture. A summary of  $^1\text{H}$  NMR spectra from these experiments is shown in Fig. 7.

As shown in the  $^1\text{H}$  NMR spectra, G-quadruplexes from **1a**, **1b** and **1c** started to dissociate in mixed solvents containing 20%  $\text{DMSO-d}_6$ . Compared with the reported  $\text{G}_{16}$ -hexadecamer from **1a**,<sup>46</sup> the  $\text{G}_8$ -octamer formed by **1b** and **1c** showed comparable stability in 20%  $\text{DMSO-d}_6$ . Eventually, all three G-quadruplexes gave complete dissociation in 50%  $\text{DMSO-d}_6$  solution with only one set of signals corresponding to the monomer. In contrast,  $[(\mathbf{1d})_4\text{K}]^+(\text{Pic}^-)$  showed significantly improved stability, with only 2% complex dissociation in 50%  $\text{DMSO-d}_6$ . This result demonstrates the significantly enhanced stability of G-quadruplexes constructed by **1d**.

To quantify the thermodynamic stability of G-quadruplexes,<sup>47</sup> VT NMR experiments were carried out for pure complexes of  $[(\mathbf{1a})_{16}\text{K}_4]^{4+} \cdot (\text{Pic}^-)_4$ ,  $[(\mathbf{1b})_8\text{K}]^+(\text{Pic}^-)$ ,  $[(\mathbf{1c})_8\text{K}]^+(\text{Pic}^-)$ , and  $[(\mathbf{1d})_4\text{K}]^+(\text{Pic}^-)$  in  $\text{CDCl}_3/\text{DMSO-d}_6$  with a fraction of 20%  $\text{DMSO-d}_6$ . The values of complex dissociation enthalpy and entropy for each G-quadruplex were calculated from van't Hoff plots and are compared in Table S6 (see detailed discussion in the ESI<sup>†</sup>). For complex  $[(\mathbf{1d})_4\text{K}]^+(\text{Pic}^-)$ , no significant increase in monomer concentration was observed with the increase in temperature. This might be attributed to the high kinetic barrier for G-quadruplex  $[(\mathbf{1d})_4\text{K}]^+(\text{Pic}^-)$  dissociation. To confirm this hypothesis, a NOESY experiment at 50 °C was performed for  $[(\mathbf{1b})_8\text{K}]^+(\text{Pic}^-)$ ,  $[(\mathbf{1c})_8\text{K}]^+(\text{Pic}^-)$  and  $[(\mathbf{1d})_4\text{K}]^+(\text{Pic}^-)$  (Fig. S14–S16<sup>†</sup>). The results suggested that kinetic exchange between the complex and monomer for  $[(\mathbf{1d})_4\text{K}]^+(\text{Pic}^-)$  was too slow to be recorded by NMR spectroscopy.

In addition to DMSO titration, the stability of  $\text{G}_8$  and  $\text{G}_{16}$  complexes could also be evaluated using tandem-MS by

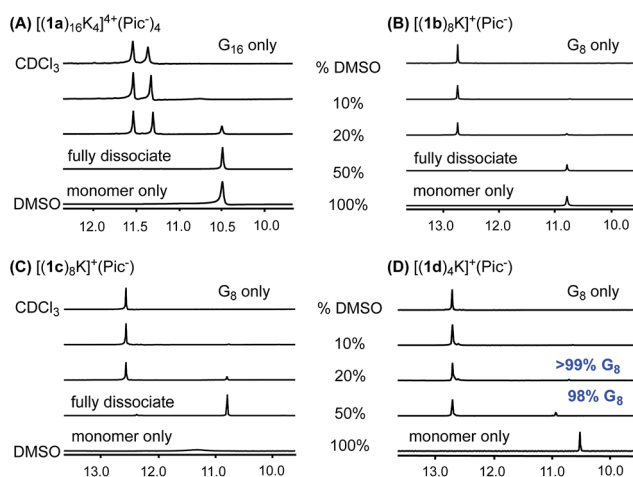


Fig. 7 DMSO- $\text{d}_6$  titration:  $^1\text{H}$  NMR spectra of (A)  $[(\mathbf{1a})_{16}\text{K}_4]^{4+} \cdot (\text{Pic}^-)_4$ , (B)  $[(\mathbf{1b})_8\text{K}]^+(\text{Pic}^-)$ , (C)  $[(\mathbf{1c})_8\text{K}]^+(\text{Pic}^-)$ , (D)  $[(\mathbf{1d})_4\text{K}]^+(\text{Pic}^-)$  in  $\text{CDCl}_3$ - $\text{DMSO-d}_6$  with  $\text{DMSO-d}_6$  fractions of 10%, 20% and 50%.

Table 2 Decomposition voltage

	$[(\mathbf{1a})_8\text{Ba}]^{2+}$	$[(\mathbf{1b})_8\text{Ba}]^{2+}$	$[(\mathbf{1c})_8\text{Ba}]^{2+}$	$[(\mathbf{1d})_4\text{Ba}]^{2+}$
Start <sup>a</sup>	30 V	40 V	50 V	70 V
End <sup>a</sup>	40 V	45 V	65 V	80 V

<sup>a</sup> Operating voltage (V).

increasing the operating voltage. The cation fragments of G-quadruplexes were separated and treated with increasing voltage. The operating voltage for G-quadruplex cation fragment decomposition are summarized in Table 2.

It is noteworthy that  $[(\mathbf{1a})_{16}\text{Ba}_2]^{4+} \cdot (\text{Pic}^-)_4$  only showed a doubly charged peak at  $m/z = 2123.31$  corresponding to  $[(\mathbf{1a})_8\text{Ba}]^{2+}$ , indicating that the picrate bridge dissociated under the MS conditions. Further comparison of all the cation fragments of the G-quadruplexes revealed a clear stability trend as  $[(\mathbf{1d})_4\text{Ba}]^{2+} > [(\mathbf{1c})_8\text{Ba}]^{2+} > [(\mathbf{1b})_8\text{Ba}]^{2+} > [(\mathbf{1a})_8\text{Ba}]^{2+}$ . Overall, the covalent linking strategy significantly helped to stabilize the  $\text{G}_8$ -octamer, both in H-bond competitive solvents and gas phase.

## Conclusions

In summary, with modification on both guanine (8-aryl) and ribose (sterically hindered 2',3' position), a stable  $\text{G}_8$ -octamer was formed with its structure characterized by single crystal X-ray diffraction for the first time. Through the analysis of cross-layer interactions, a covalently tethered 8-aryl guanosine dimer was designed and prepared for supramolecular assembly. The expected  $\text{G}_8$ -octamer was confirmed by X-ray, MS and NMR spectroscopy with significantly improved stability in MeOH and 1 : 1  $\text{DMSO}/\text{CDCl}_3$  mixture. To the best of our knowledge, this is the first example of discrete G-quadruplexes formed from small molecules with enhanced stability in a protic solvent (MeOH) and a polar aprotic solvent (DMSO). Meanwhile, formation of the stable  $\text{G}_8$ -octamer with a concise and well-defined bottom-to-bottom stacking mode provides a novel supramolecular platform. Incorporation of this new system into material and biological applications is expected and currently undergoing in our group.

## Conflicts of interest

There are no conflicts to declare.

## Acknowledgements

We are grateful to the NSF (CHE-1665122), the NIH (1R01GM120240-01), and NSFC (21629201) for financial support.

## Notes and references

§ All the structures reported in this article have been deposited with the Cambridge Crystallographic Data Centre. The accession numbers for  $[(\mathbf{1b})_8\text{Ba}]^{2+} \cdot (\text{Pic}^-)_2$ ;  $[(\mathbf{1b})_8\text{K}]^+(\text{PF}_6^-)$ ;  $[(\mathbf{1b})_8\text{K}]^+(\text{Pic}^-)$ ;  $[(\mathbf{1b})_8\text{Sr}]^{2+} \cdot (\text{Pic}^-)_2$ ;  $[(\mathbf{1b})_8\text{Rb}]^+(\text{Pic}^-)$ ;  $[(\mathbf{1c})_8\text{Ba}]^{2+} \cdot (\text{Pic}^-)_2$ ;  $[(\mathbf{1d})_4\text{K}]^+(\text{Pic}^-)$  reported in this paper are:



1871565, 1871566, 1871567, 1871568, 1871569, 1871570, 1871754, correspondingly.

- 1 M. Fujita, *Structure and Bonding*, Springer, Berlin, 2000, pp. 177–201.
- 2 D. S. Lawrence, T. Jiang and M. Levett, *Chem. Rev.*, 1995, **95**, 2229–2260.
- 3 D. P. Craig and D. P. Mellor, *Structure and Bonding*, Springer, Berlin, 1976, pp. 1–48.
- 4 M. Fujita, *Chem. Soc. Rev.*, 1998, **27**, 417–425.
- 5 L. J. Prins, D. N. Reinhoudt and P. Timmerman, *Angew. Chem., Int. Ed.*, 2001, **40**, 2382–2426.
- 6 P. Y. W. Dankers and E. W. Meijer, *Bull. Chem. Soc. Jpn.*, 2007, **80**, 2047–2073.
- 7 H.-W. Jun, S. E. Paramonov and J. D. Hartgerink, *Soft Matter*, 2006, **2**, 177–181.
- 8 P. Xin, P. Zhu, P. Su, J.-L. Hou and Z.-T. Li, *J. Am. Chem. Soc.*, 2014, **136**, 13078–13081.
- 9 J. T. Davis, *Angew. Chem., Int. Ed.*, 2004, **43**, 668–698.
- 10 J. L. Sessler, C. M. Lawrence and J. Jayawickramarajah, *Chem. Soc. Rev.*, 2007, **36**, 314–325.
- 11 C. L. D. Gibb and B. C. Gibb, *J. Am. Chem. Soc.*, 2004, **126**, 11408–11409.
- 12 G. V. Oshovsky, D. N. Reinhoudt and W. Verboom, *Angew. Chem., Int. Ed.*, 2007, **46**, 2366–2393.
- 13 J. T. Davis and G. P. Spada, *Chem. Soc. Rev.*, 2007, **36**, 296–313.
- 14 G. P. Spada and G. Gottarelli, *Synlett*, 2004, **4**, 596–602.
- 15 E. Bouhoutsos-Brown, C. L. Marshall and T. J. Pinnavaia, *J. Am. Chem. Soc.*, 1982, **104**, 6576–6584.
- 16 J. P. N. V. Hud, *Quadruplex Nucleic Acids*, The Royal Society of Chemistry, Cambridge, 2006, pp. 100–130.
- 17 J. A. Walmsley, R. G. Barr, E. Bouhoutsos-Brown and T. J. Pinnavaia, *J. Phys. Chem.*, 1984, **88**, 2599–2605.
- 18 G. Biffi, M. Di Antonio, D. Tannahill and S. Balasubramanian, *Nat. Chem.*, 2013, **6**, 75.
- 19 J. N. Parkinson, *Quadruplex Nucleic Acids*, The Royal Society of Chemistry, Cambridge, 2006, pp. 1–30.
- 20 M. Zeraati, D. B. Langley, P. Schofield, A. L. Moye, R. Rouet, W. E. Hughes, T. M. Bryan, M. E. Dinger and D. Christ, *Nat. Chem.*, 2018, **10**, 631–637.
- 21 I. C. M. Kwan, Y.-M. She and G. Wu, *Can. J. Chem.*, 2011, **89**, 835–844.
- 22 M. a. D. C. Rivera-Sánchez, M. García-Arriaga, G. Hogley, A. V. Morales-de-Echegaray and J. M. Rivera, *ACS Omega*, 2017, **2**, 6619–6627.
- 23 M. d. C. Rivera-Sánchez, I. Andújar-de-Sanctis, M. García-Arriaga, V. Gubala, G. Hogley and J. M. Rivera, *J. Am. Chem. Soc.*, 2009, **131**, 10403–10405.
- 24 R. N. Das, Y. P. Kumar, O. M. Schütte, C. Steinem and J. Dash, *J. Am. Chem. Soc.*, 2015, **137**, 34–37.
- 25 S. L. Forman, J. C. Fettingner, S. Pieraccini, G. Gottarelli and J. T. Davis, *J. Am. Chem. Soc.*, 2000, **122**, 4060–4067.
- 26 M. S. Kaucher, W. A. Harrell and J. T. Davis, *J. Am. Chem. Soc.*, 2006, **128**, 38–39.
- 27 T. Bhattacharyya, P. Saha and J. Dash, *ACS Omega*, 2018, **3**, 2230–2241.
- 28 G. M. Peters and J. T. Davis, *Chem. Soc. Rev.*, 2016, **45**, 3188–3206.
- 29 G. M. Peters, L. P. Skala and J. T. Davis, *J. Am. Chem. Soc.*, 2016, **138**, 134–139.
- 30 M. García-Iglesias, T. Torres and D. González-Rodríguez, *Chem. Commun.*, 2016, **52**, 9446–9449.
- 31 D. González-Rodríguez, P. G. A. Janssen, R. Martín-Rapún, I. D. De Cat, S. De Feyter, A. P. H. J. Schenning and E. W. Meijer, *J. Am. Chem. Soc.*, 2010, **132**, 4710–4719.
- 32 H. Han and L. H. Hurley, *Trends Pharmacol. Sci.*, 2000, **21**, 136–142.
- 33 F. W. B. Van Leeuwen, W. Verboom, X. Shi, J. T. Davis and D. N. Reinhoudt, *J. Am. Chem. Soc.*, 2004, **126**, 16575–16581.
- 34 J. E. Betancourt, C. Subramani, J. L. Serrano-Velez, E. Rosamolinar, V. M. Rotello and J. M. Rivera, *Chem. Commun.*, 2010, **46**, 8537–8539.
- 35 S. Martić, G. Wu and S. Wang, *Inorg. Chem.*, 2008, **47**, 8315–8323.
- 36 J. M. Rivera, M. Martín-Hidalgo and J. C. Rivera-Ríos, *Org. Biomol. Chem.*, 2012, **10**, 7562–7565.
- 37 J. M. Rivera and D. Silva-Brenes, *Org. Lett.*, 2013, **15**, 2350–2353.
- 38 M. Martín-Hidalgo and J. M. Rivera, *Chem. Commun.*, 2011, **47**, 12485–12487.
- 39 K. B. Sutyak, P. Y. Zavalij, M. L. Robinson and J. T. Davis, *Chem. Commun.*, 2016, **52**, 11112–11115.
- 40 J. E. Betancourt, M. Martín-Hidalgo, V. Gubala and J. M. Rivera, *J. Am. Chem. Soc.*, 2009, **131**, 3186–3188.
- 41 D. González-Rodríguez, J. L. J. van Dongen, M. Lutz, A. L. Spek, A. P. H. J. Schenning and E. W. Meijer, *Nat. Chem.*, 2009, **1**, 151–155.
- 42 J. E. Betancourt and J. M. Rivera, *J. Am. Chem. Soc.*, 2009, **131**, 16666–16668.
- 43 J. E. Betancourt and J. M. Rivera, *Org. Lett.*, 2008, **10**, 2287–2290.
- 44 V. Gubala, J. E. Betancourt and J. M. Rivera, *Org. Lett.*, 2004, **6**, 4735–4738.
- 45 S. B. Zimmerman, *J. Mol. Biol.*, 1976, **106**, 663–672.
- 46 X. Shi, K. M. Mullaugh, J. C. Fettingner, Y. Jiang, S. A. Hofstadler and J. T. Davis, *J. Am. Chem. Soc.*, 2003, **125**, 10830–10841.
- 47 E. Fadaei, M. Martín-Arroyo, M. Tafazzoli and D. González-Rodríguez, *Org. Lett.*, 2017, **19**, 460–463.
- 48 M. García-Arriaga, G. Hogley and J. M. Rivera, *J. Am. Chem. Soc.*, 2008, **130**, 10492–10493.
- 49 A. L. Marlow, E. Mezzina, G. P. Spada, S. Masiero, J. T. Davis and G. Gottarelli, *J. Org. Chem.*, 1999, **64**, 5116–5123.
- 50 M. García-Arriaga, G. Hogley and J. M. Rivera, *J. Org. Chem.*, 2016, **81**, 6026–6035.
- 51 S. Lena, P. Neviani, S. Masiero, S. Pieraccini and G. P. Spada, *Angew. Chem., Int. Ed.*, 2010, **49**, 3657–3660.
- 52 S. Marti, X. Liu, S. Wang and G. Wu, *Chem.–Eur. J.*, 2008, **14**, 1196–1204.
- 53 X. Meng, T. Moriuchi, M. Kawahata, K. Yamaguchi and T. Hirao, *Chem. Commun.*, 2011, **47**, 4682–4864.
- 54 J. L. Sessler, M. Sathiosatham, K. Doerr, V. Lynch and K. A. Abboud, *Angew. Chem., Int. Ed.*, 2000, **39**, 1300–1303.



- 55 X. Shi, J. C. Fettinger and J. T. Davis, *Angew. Chem., Int. Ed.*, 2001, **40**, 2827–2831.
- 56 X. Shi, J. C. Fettinger and J. T. Davis, *J. Am. Chem. Soc.*, 2001, **123**, 6738–6739.
- 57 H. Wang, X. Qian, K. Wang, M. Su, W.-W. Haoyang, X. Jiang, R. Brzozowski, M. Wang, X. Gao, Y. Li, B. Xu, P. Eswara, X.-Q. Hao, W. Gong, J.-L. Hou, J. Cai and X. Li, *Nat. Commun.*, 2018, **9**, 1815.
- 58 J. G. Speight, *Lange's Handbook of Chemistry*, McGraw-Hill, New York, 16th edn, 2005, pp. 1–150.
- 59 R. Ida and G. Wu, *Chem. Commun.*, 2005, 4294–4296.

